Telescope Aiming Point Tracking Method for Bioptic Driving Surveillance

Xianping Fu, Gang Luo, and Eli Peli, *Member, IEEE*

Abstract—A bioptic telescope is a visual aid used by people with impaired vision when driving in many U.S. states, though bioptic driving remains controversial. Objective data on how and when bioptic drivers use the telescope and what they look at with it are crucial to understanding the bioptic telescope's effects on driving. A video-based technique to track the telescope's aiming point is presented in this paper. With three infrared retro-reflective markers pasted on the bioptic spectacles frame, its movement is recorded using an infrared camera unit with infrared LED illuminators. The angles formed by the three markers are used to calculate the telescope's aiming points, which are registered with road scene images recorded by another camera. The calculation is based on a novel one-time calibration method, in which the light spot from a head-mounted laser pointer projected on a wall while the scanning is recorded by the scene camera, in synchronization with the infrared camera. Interpolation is performed within small local regions where no samples were taken. Thus, non-linear interpolation error can be minimized, even for wide-range tracking. Experiments demonstrated that the average error over a $70° \times 48°$ field was only $0.86°$, with lateral head movement allowed.

Index Terms—Bioptic driving, head tracking, instrumented vehicle, low vision, vision rehabilitation.

I. INTRODUCTION

WITH increasing longevity, age-related vision loss is rising. Based on the 2000 U.S. Census, an estimated 2.4 million American adults have low vision (best corrected visual acuity worse than 20/40), typically caused by conditions such as age-related macular degeneration, optic atrophy and diabetic retinopathy [1]. Because of failure to meet the vision screening requirements for licensing, many people lose their driving privileges, which results in restricted mobility and negative impact on the quality of life. Spectacle-mounted bioptic telescopes [Fig. 1(a)] were introduced in the early 1950s as a visual aid for people with impaired vision, and have been used as driving aid since the 1960s. The magnification provided by the telescope compensates for reduced visual acuity.

Currently, people with moderately impaired vision can legally drive with a bioptic telescope in 39 U.S. states [2] and as of 2009 also in The Netherlands. Most of the time, the users view and scan the environment through the carrier spectacle lenses, with an unrestricted field of vision [Fig. 1(b), left]. With a slight downward head tilt, they spot intermittently through the telescope [Fig. 1(b) right and (c)] to read road signs, determine the status of traffic lights, or scan ahead for road hazards [3]. A brief glance (recommended to be 1–2 s) through the telescope provides the user with the required high-resolution information needed to recognize details.

Although it is a legal option, whether the use of bioptic telescopes results in better (or worse) driving performance remains controversial [4], [5]. Both proponents and opponents agree the bioptic has optical limitations; one of which is an optically-induced ring scotoma. When viewing through the telescope, the magnified field occupies a larger retinal area than the nonmagnified field by the factor of the telescope magnification. This creates a blind area or ring scotoma around the field-of-view through the telescope. It is not known whether accidents involving bioptic drivers occurred when looking through the narrow field of the telescope (which might obscure relevant traffic) [Fig. 1(c)] or occurred because of failure to look through the telescope (which might result in poor perception of important traffic signs or other detailed information). Collecting data on when bioptic drivers view through the telescope and what they see through it in actual daily driving activities is crucial to address these issues [6]–[8].

We built an in-car surveillance system to record bioptic drivers' routine driving activities. The system continuously records video of the bioptic telescope position and video of the road scene. In addition, the system records "black box" car data such as acceleration, speed, brake usage and turn signals, and GPS coordinates. Recordings are captured by a trunk-mounted digital video recorder (DVR) for later interpretation. The system can operate unattended for months. Recordings are processed semi-automatically to cull the thousands of hours of recordings and identify segments to be shown to expert driving evaluators who will assess the use of the bioptic telescopes and the performance of the drivers. The video recordings can be used to identify head tilt actions, and thus flag the segments incorporating bioptic telescope use. The ability to automatically estimate the telescope's aiming point allows us to show the evaluators the targets that the drivers viewed through the telescope. We define the aiming point as the intersection point between the telescope axis and the scene-camera image plane. That is, the telescope aiming point is at the center of the magnified field-of-view of the telescope [Fig. 1(c)]. We
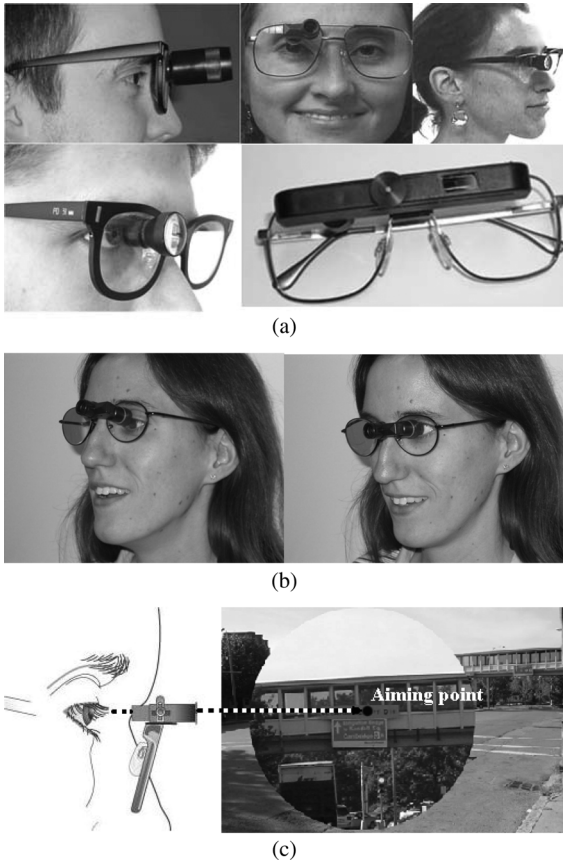
Fig. 1. Bioptic telescopes used for driving. (a) Some typical bioptic telescopes used for driving. (b) Most of the time the wearer views through the carrier lens (under the telescope) without any effect of the telescope (left). With a slight downward tilt of the head, the telescope is brought into the line of sight, providing a magnified view of the object of interest (right). (c) The line of sight and tube of telescope are aligned when driver looks straight through the telescope. (Illustration on left from http://www.biopticdriving.org.) The aiming point is located at the center of the magnified view of the telescope, although the driver may actually be looking anywhere within the telescope field-of-view that may span 10°–15°.

needed a robust way to determine aiming point based on a calibration procedure that could be performed for each driver's telescope and car once, and requires no further calibration each time the car is driven. This paper presents the development and validation of our calibration method for deriving the aiming point.

Our determination of the telescope aiming point on the scene images needs to be accurate enough for a driving evaluator to judge what the driver was viewing through the telescope. Given the recording resolution of our system, features subtending as little as 2° of visual angle can generally be distinguished in the scene camera image, so an aiming point accuracy on the order of 1° would place the calculated aiming point within most features. It is possible, however, for drivers to spot targets anywhere within the telescope's field, typically about 10°–15° in diameter, and if there is more than one target within the field there is no way we can determine which is the intended target. However, image quality falls off with distance from the telescope aiming point, so it is likely that once a target is spotted, the wearer will center the aiming point close to it.

Because studies of normal daily driving usually require minimal attachment of tracking apparatus, video-based tracking methods [9]–[13] are usually more suitable for head tracking than those based on worn sensors. Feature detection is the first step in video-based techniques. Feature detection can be based on natural facial features [11], [14], [15] or fiducial markers placed on the face or head. Precise tracking of facial features is difficult their locations can easily be altered by changing expressions, such as laughing and talking, as well as changes in facial hair and eyewear. We found that most existing face-based approaches either added considerable complexity to our application or were not accurate enough for our bioptic driving study.

Fiducial marker tracking is a simple, robust, and accurate approach that is widely used in many practical applications [16], for example, NaturalPoint Track IR (NaturalPoint, Inc., Corvallis, OR) for video games. Fiducial markers must be rigidly associated with head position (or, in our case, telescope position) to avoid the same limitations as face-based features. Markers mounted directly on the spectacle frames do not have that problem, and are easily detected automatically. That is our chosen method.

We pasted infrared retro-reflective markers onto the user's spectacle frame. Used together with an infrared (IR) band-pass filter on the camera, the markers' visibility remains stable in the real world driving environment, where illumination and shading may dramatically change. Once markers are detected, it is necessary to determine the relationship between the markers and their position and orientation in space, and from that, determine the aiming point of the telescope. Typically, the user needs to aim his gaze at some indicated calibration points, generally arrayed in a grid across the scene, while at the same time the image of the markers is recorded. Usually, calibration is performed indoors and the calibration points are on a screen. Carefully aiming at numerous points can become tedious and is error prone. A lengthy and cumbersome calibration procedure may be especially difficult for people with impaired vision and advanced age, as in our target population. The number of points needed can be reduced by using multiple cameras and IR illumination, but that increases system cost and complexity [17]. The solution we developed overcomes these limitations.

In our application, it may be difficult to track the driver's eye movements, because the telescope often occludes the camera's view of the eye [Fig. 1(a)]. Fortunately, that is not necessary, as we know that when the user is looking through the telescope, the telescope's aiming point is along the telescope axis, and the driver's field-of-view is constrained to be within the telescope's field. Therefore, in order to determine what the driver is looking at through the telescope, it is sufficient to just track and calibrate the aiming of the telescope. Even changes in position of spectacle frame on the face do not affect the tracking, as the users always look where the telescope points. Because of this, we argue that the system can be calibrated by an experimenter wearing the subject's bioptic telescope, and the calibration will still be valid for the subject bioptic driver. This simplifies the calibration process for the visually impaired subjects and ensures that the calibration is performed properly. We have verified this, as described below.

For most types of bioptic telescopes, the telescope is rigidly mounted in the frame. Thus, tracking the spectacle frame is sufficient. For a frame-mounted type of telescope [such as the Ocutech VHS, lower-right in Fig. 1(a)], there could be some position variability between the frame and telescope after fitting. However, we do not expect the variability to be a problem, as a strong locking mechanism is available. In addition, in some states this type of telescope is not permitted for driving as it blocks the view of the fellow eye when the user is looking through the telescope.

We developed a novel calibration method that is robust, flexible, and trivially easy for the visually-impaired subject, as it can be accomplished without the subject by an experimenter in the subject's car, wearing the subject's telescopic spectacles. Ours is a wide-field calibration method in which a large number of calibration points located across the scene field can be easily obtained and applied to estimate the aiming point.

II. METHOD

A. Bioptic Driving Surveillance System

We have developed an in-car recording system [18] that is comprised of a mobile DVR system that records multiple video channels, including images of the road scene and the driver's head (Fig. 2). A wide-angle camera is mounted forward of the rearview mirror to capture the road and traffic scene. A band-pass IR camera is mounted on the windshield on the driver's side to capture IR-reflective fiducial markers on the driver's spectacle frame, to track the telescope aiming point. A third camera (behavior camera) is mounted on the far right side of the windshield to capture the driver's head and body movements, to aid experimenters in assessing driver actions and confirm the bioptic use (by checking if the iris is aligned with the telescope tube).

B. In-Car Telescope Aiming Point Tracking

Tracking the telescope aiming point is achieved by tracking the frame of the driver's bioptic spectacles. The frame tracking provides information about head movement (to supplement the detection of telescope usage by noting head tilt) as well as the aiming point through the telescope. Actual position of the spectacles on the driver's face is not important, since the driver must be looking through the telescope when using it. Shifting frame position and slips in its location on the nose can be tolerated, as they negligibly affect determining the location of a distant aiming point. Therefore, once the spectacle frame is calibrated in the car by one person, such as the experimenter, the calibration is valid no matter who wears the frame in driving, as long as the camera position remains stable. This means that our tracking method may be calibration-free for the visually impaired subjects in our study, and is not sensitive to minor changes such as driver seat adjustment or postural changes.

In order to acquire reliable video images in actual driving situations, where ambient light levels change dramatically between night and direct sunlight and sharp shadows can appear across the face, we used a near-IR camera, with an 850–900 nm band-pass filter, aimed at the driver's head to capture images. Three retro-reflective markers were pasted on the front of
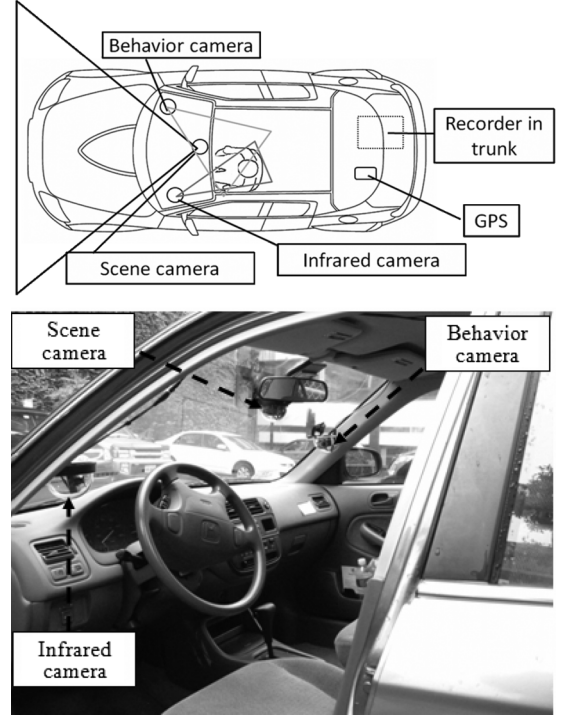

Fig. 2. The digital in-car surveillance system is comprised of a wide-scene camera (or two side-by side cameras) mounted behind the rearview mirror and aimed at the road ahead, and two cameras aimed at the driver. One, an IR camera with an IR illuminator (on the left), is used to detect head orientation and thus, telescope usage and line of sight. The second, on the far right, is used to monitor driving behavior, and to verify that a head down tilt detected by the IR camera is really for telescope use.

the driver's bioptic spectacle frame [Fig. 3(a)]. These reflectors are illuminated by 890 nm IR LEDs mounted with the camera. This imaging system suppresses changes in the ambient light. The IR illumination is not visible to the driver, and therefore does not interfere with driving. A captured image of a bioptic driver's head and the reflective markers is shown in Fig. 3(b). The three markers in these IR images can be detected robustly even under wide variations in lighting conditions. Direct bright sunlight can swamp the marker images, but drivers do not tolerate direct sunlight in their eyes, and use the visors to keep their eyes, and thus the spectacle frame, will be kept in shadow. The telescope aim is rigidly linked to the triangle formed by the three markers [Fig. 3(c)]. The shape of the triangle, formed by the three markers, changes with head yaw (left–right) and pitch (up–down), but it is less sensitive to lateral head movement, as the results below show. The size of the triangle can change slightly with distance of the head from the camera, but this does not materially affect pointing direction. The telescope aiming point therefore can be calculated using two angles of the triangle to represent the triangle's shape. With the IR camera located to the left–front of the driver, the captured triangle shape changes with head rotation. Thus, the three markers are used as feature points to track the telescope's aiming point.

C. Calibration for Telescope Aiming Point

In our application, the system in the car has to be simple, yet many calibration points are needed to ensure accuracy over the

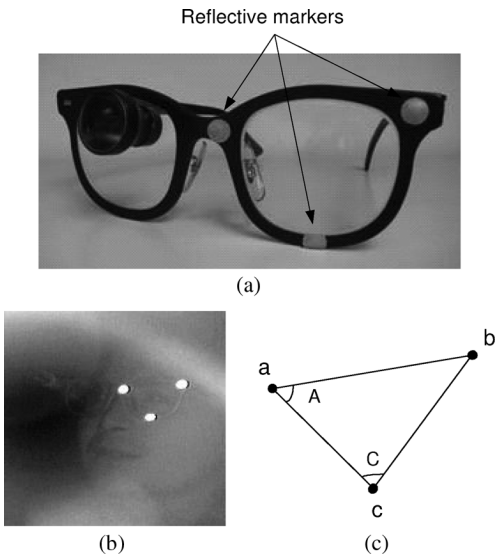(a)

(b)   (c)

Fig. 3. (a) Reflective markers mounted on the bioptic spectacle frame. (b) IR image of a bioptic driver's head showing the IR-illuminated retro-reflecting markers. (c) Frame movements caused by head yaw and pitch are reflected in the shape of the triangle formed by the markers. Specifically, we used angles A and C to determine the telescope aiming point.

wide range of head movement common in driving, and where the wide scene image is highly distorted by the wide-angle lens of the scene camera, and the distance from the scene camera to observed objects in real driving situations is highly variable. Because we only need to associate head yaw and pitch values with points in the 2-D scene images, in this situation direct interpolation based on scene images provides a simple solution. For calibration, we mounted a laser pointer on the spectacle temple to project a light spot on a distant wall in view of the scene camera. The light spot's location is arbitrary, but it can easily be located in the scene image by means of image processing. Moving the head to scan over the scene while recording the head and scene images provides a long trail of calibration points. Thus, we easily record a copious number of calibration points across the scene, without involving the actual driver and without requiring repetitive and careful aiming by the experimenter.

As illustrated in Fig. 4, calibration is performed in front of a wall (the "calibration plane," typically about 5 m away). The laser pointer is adjusted on the spectacle frame temple so that the laser spot coincides with the telescope aiming point on the wall, thus almost completely compensating for the parallax between the telescope and laser at that distance. During the calibration, the bioptic wearer freely moves his head to scan the scene field with the laser spot. The videos of head and scene are recorded in synchronization. Thus, the light spot position on the scene image and reflective marker positions are paired for each video frame.

Fig. 5 illustrates the different shapes of the marker triangle at nine (out of thousands) different telescope aiming points in the scene image. We used nonlinear surface fitting to establish the relationship between aiming points and the triangle shapes determined from the angle pairs (A, C). The inverse of that re-
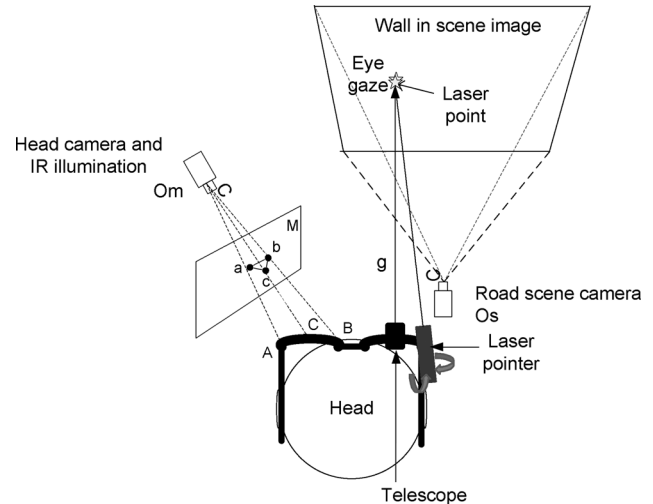

Fig. 4. Illustration of wide-field calibration without fixed calibration points. A head-mounted laser pointer projects a light spot, which serves as a floating calibration point, on a wall (the calibration plane). The IR camera that is aimed at the head, captures the image of the reflectors on the spectacle frame, and a scene camera captures the image of the light spot. When the person moves his head to scan the light spot across the whole field, a large number of calibration points can be obtained rapidly (one for each video frame).
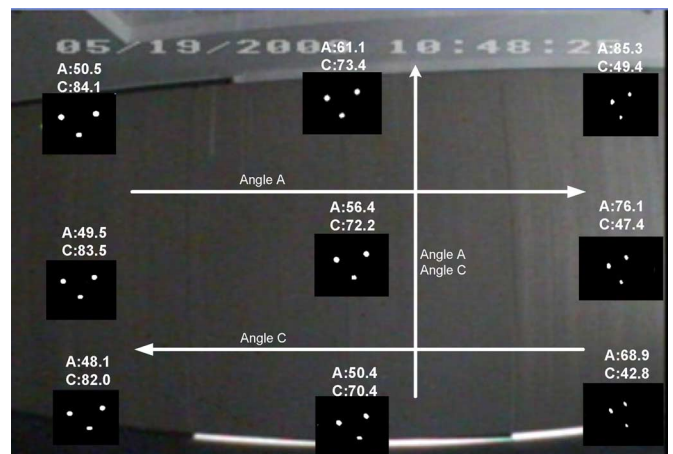

Fig. 5. Illustration of the relationship between the telescope aiming point and the triangle-shaped markers configuration. Each triangular image inset is placed at the corresponding aiming point location on the scene image of the wall used for calibration. Movements in the directions shown by the arrows increase the size of the angle(s) labeling the arrows.

lationship can then be used, via interpolation, to identify the aiming point from any given angle pair within the field.

D. Parallax Error Analysis

Calibration is performed using a calibration plane (wall) at a fixed distance, typically about 5 m. The estimate of aiming point location derived for this distance will deviate for objects at different distances due to the lateral parallax between the telescope and scene camera. Because the distance to observed objects in real driving situations is usually unknown, this is a systematic error that cannot be corrected easily. The magnitude and impact of this scene camera parallax error is analyzed in this section.

In the car, the scene camera is mounted at the back of the rearview mirror so it does not obstruct the driver's view of the roadway (Fig. 2). This installation creates parallax between the
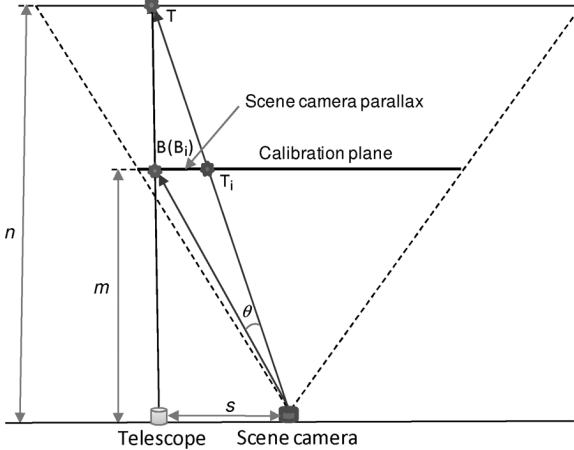
Fig. 6. The scene camera parallax. When the target moves from B to T, the telescope aiming point remains the same (and angle pair A and C are same), but the view of the target in the scene image moves from Bi to Ti. The error from Bi to Ti is due to scene camera parallax that is determined by the lateral distance from scene camera to telescope, s, the calibration distance, m, and the target distance, n. Horizontal scale is exaggerated in this figure.
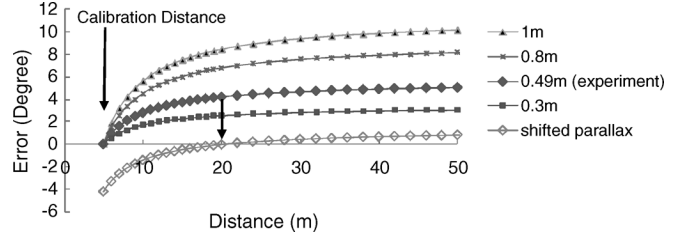

Fig. 7. The systematic errors caused by the scene camera parallax for different target distances, assuming a calibration distance of 5 m. Errors for 0.3, 0.49, 0.8, and 1 m parallax are calculated. The error is $4.9°$ for targets at 50 m and 0.49 m parallax. The aiming point calculation can be biased to reduce the error over a large range of depths. A curve shifted to null the error at 20 m (open diamond symbols) shows that for greater distance, where targets subtending small angles are more prevalent, reduces their error to less than $1°$. Larger errors occur closer in; where targets subtend larger angles and the indicated aiming point would likely still fall within the target object (only few relevant targets in driving appear at such short distances).

bioptic telescope and the scene camera. As illustrated in Fig. 6, for two targets at different distances along the telescope's line of sight, the telescope's aiming direction is the same but their positions in the scene camera's image are different. For example, target B and target T have the same telescope direction (and thus the same recorded marker triangle shape), but their images in the scene camera (B_i and T_i) are separated. Using the mapping relationship between marker angles and scene camera image coordinates that was established with points lying on the calibration plane, this telescope direction is mapped correctly to target B's location in the scene image (B_i). When target is at position T, however, its image in the scene camera (T_i) is displaced from the predicted scene image coordinates. Thus there is an angular error in the identified position of any targets not on the calibration plane. This parallax error can be computed (for targets along a line of sight perpendicular to the calibration plane) as

$$\theta = \tan^{-1}\left(\frac{s}{m}\right) - \tan^{-1}\left(\frac{s}{n}\right) \qquad (1)$$

where s is the lateral distance from the scene camera to the telescope, m is the calibration distance (calibration plane from telescope), and n is the distance from telescope to targets that are not on the calibration plane. The forward distance between the telescope and camera (a few tens of cm) is negligible compared to the distance to the targets (many meters), and so it is not included in this approximation.

Fig. 7 shows the computed errors for targets at different distances, assuming the calibration distance, m, is 5 m and s is 0.3, 0.49, 0.8, or 1 m. A scene camera parallax of 0.49 m is approximately the case for many vehicles, including the car we have instrumented. For that offset, when the calibration distance is 5 m and the target distance is 50 m, scene camera parallax error is about $4.9°$, which would not be acceptable. Since most telescope-relevant targets in driving are at much larger distances than 5 m, the impact of parallax error may be reduced by performing the calibration at a farther distance. The calibration plane, however, may not be practically set very far. It

is restricted by the availability of a large enough wall spanning the wide field-of-view needed while driving (wider than a highway) and by the need of a laser pointer which produces a spot reflection bright enough to be picked up by the scene camera. Although the actual target distance is usually unknown, the trend of the systematic error is known, and thus the estimated aiming point can be biased to reduce the parallax error for the most common target distance. See the "shifted parallax" curve in Fig. 7, which is biased for a 20 m target distance. It can be seen that after shifting, the error at 50 m target distances is only $0.85°$.

In addition, the variability in the distance between the head and the scene camera s, which may be due to unpredictable lateral body movement of the driver, will cause random errors in aiming point estimation. Purely lateral movement is supposed to be associated with aiming point shift, but our method can not detect the change because the triangle remains unchanged. However, the error can be ignored in our application, given the confined lateral movement range in cars and the relatively large target distances. For instance, 10 cm lateral movement (most actual movements are likely smaller than 10 cm) causes an error smaller than $0.11°$ for a 50 m target distance.

III. RESULTS

Experiments were conducted in a large meeting hall, where a large calibration wall was available and target distances could be measured easily. Following a calibration procedure performed at a distance of 5 m from the wall by one subject, four experiments were conducted: 1) verification at the calibration distance without lateral head movements (only yaw and pitch); 2) verification at the calibration distance with lateral head movements; 3) estimation of aiming points for targets at distances from 5 to 20 m (where the expected errors are largest); 4) estimation of aiming point for other users (using the calibration obtained by the first subject) for targets distances from 5 to 20 m. In these experiments, the head and scene video images were 352×240 pixels, and the field-of-view of the scene camera was $70° \times 48°$.

In addition, we conducted an on-road experiment in a car with a prototype system installed.
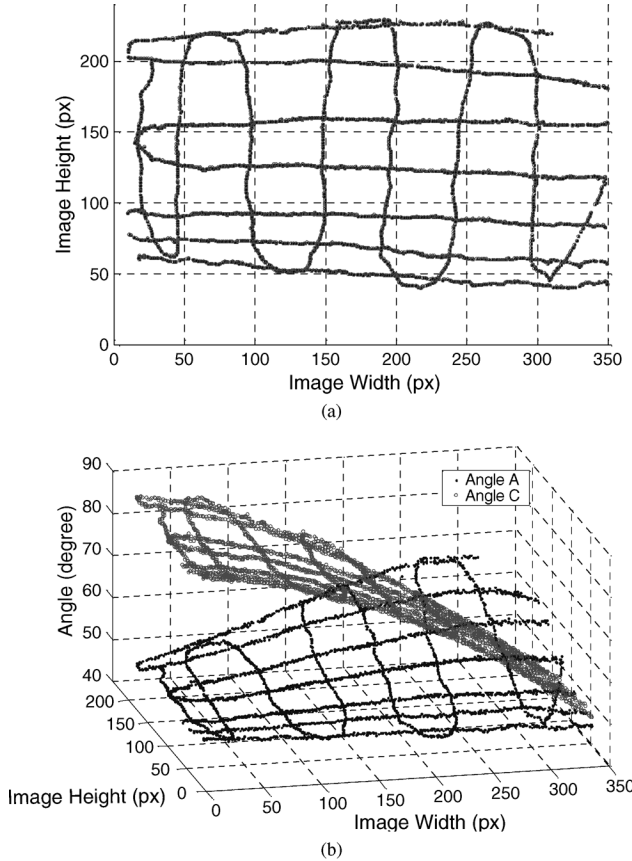
Fig. 8. (a) The trajectory of laser light spot measured from the scene camera during a full-field calibration. (b) Angle pair A and C as functions of the light spot coordinates for every laser spot location recorded.
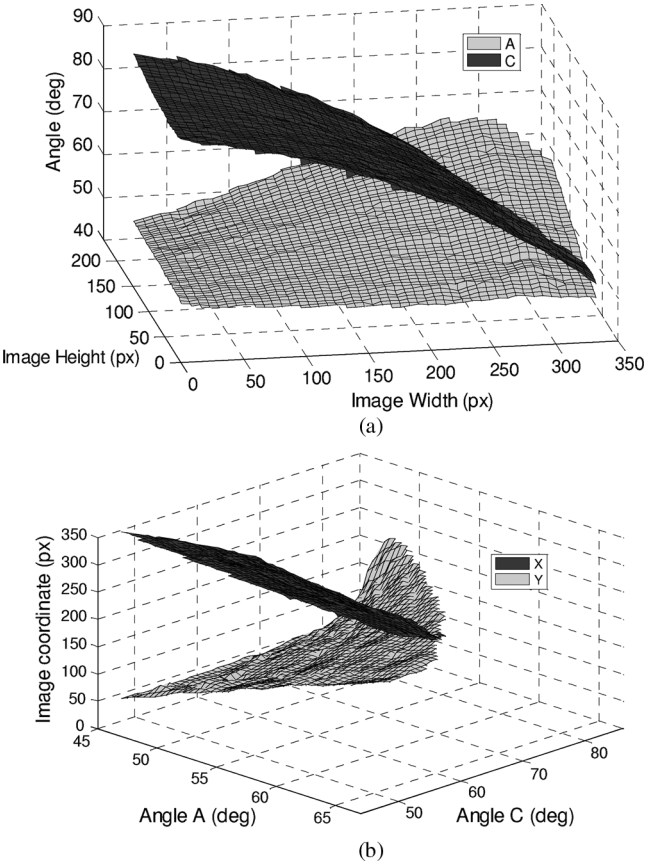

Fig. 9. The computed relationships between telescope aiming points (X, Y) in scene camera coordinates, and angle pairs (A, C) of the marker triangle. (a) The results of interpolating the data from Fig. 8(b). As each aiming point (X, Y) on the scene image corresponds to a unique pair of angles A and C, the function can be inverted. (b) The inverted interpolation function, providing a unique aiming point (X, Y) corresponding to any pair of angles A and C in the interpolated dataset.

A. Indoor Calibration

The laser pointer was adjusted to bring the laser spot to the middle of the telescope field-of-view on the calibration wall and was locked in that position. During calibration, the subject moved his head to perform raster scans across the full field of the scene camera horizontally and vertically. The trajectory of the laser light spot derived from the scene image is shown in Fig. 8(a). The angles A and C of the marker triangle obtained for each of those light spot positions derived from the IR camera signal are shown in Fig. 8(b).

Based on the collected calibration data, the angles A and C for all image pixels in the scene camera were estimated by linear interpolation. As with any interpolation, this assumes that the mapping between the shape of the triangle formed by the markers and the telescope aiming point in the scene image behaves smoothly locally. Fig. 9(a) shows the results of the interpolation. To calculate the telescope aiming points from angle pairs, a reversed interpolation from the angles (A, C) to scene coordinates (X, Y) is used [Fig. 9(b)]. This assumes the inverse is unique, which is evident by inspection of the data.

B. Verification Without Lateral Body Movement

During this verification, the subject wore the spectacles with the laser pointer positioned as during calibration, and rotated his head, without lateral shifts, to project the laser spot at different arbitrary regions on the wall. The distance between the

coordinates of the laser spot in the scene camera image and the aiming point, calculated from the calibration analysis of the triangle markers in the corresponding IR camera frame, was computed for each frame. Fig. 10 plots the laser spots and the corresponding calculated aiming points in scene camera coordinates. As can be seen, the subject moved his head to 19 arbitrary locations, and he did not hold his head absolutely still at any location. In total, we collected 310 measurement points. The largest error was 2.56°, the smallest error was 0.06°, and the average error was 1.22°.

C. Tracking With Lateral Body Movements

Lateral body movements can't be avoided in driving. To assess the magnitude of the effect of lateral body movements on the tracking method, the prior experiment was repeated with intentional body movements. For each arbitrary head rotation, the subject attempted to keep looking through the telescope at the same position while he laterally shifted his body left to right, back and forth. The movement range was about 16 cm backward and forward and 20 cm left and right.

The tracking results are shown in Fig. 11. The largest error was 3.03°, the smallest error was 0.07°, and the average error was 0.86°.
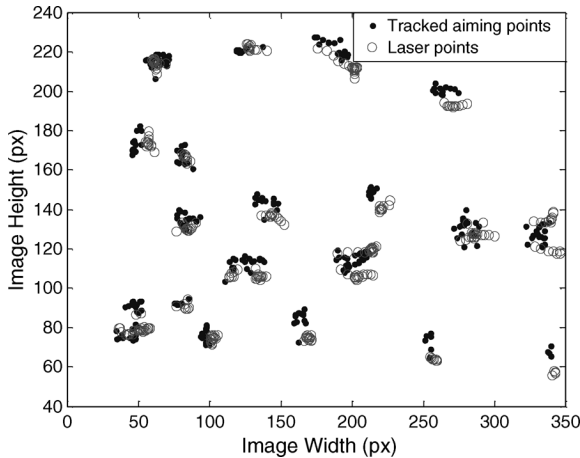
Fig. 10.   Verification of telescope's aiming point tracking without lateral body movements. Verification points (laser light spots) in the scene image (circles) and calculated tracking results (solid dots). The number of tracking points is 310; the average of error is 1.22°. The size that the field of the scene camera covers is $70° \times 48°$.
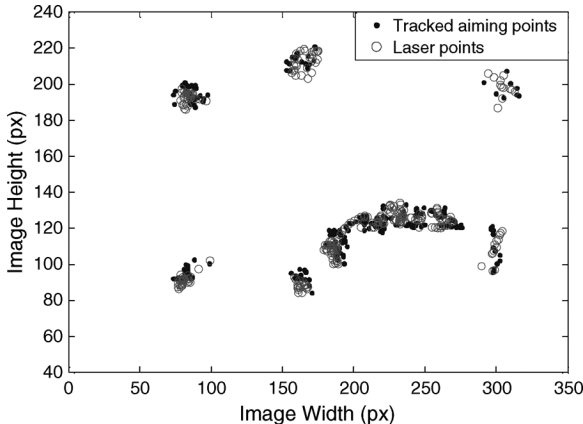

Fig. 11.   Verification of telescope's aiming point tracking with lateral body movements. Verification points (laser spots) in the scene image (circles) and tracking results (solid dots). The number of tracking points is 261; the average error is 0.86°.

Comparing Figs. 10 and 11, it is evident that when the bioptic wearer gazed at different targets with lateral body movements a smaller field area was covered with the gaze points. That is likely the reason the average error was slightly smaller in that experiment.

D.   Tracking Targets at Different Distances and With Different Subjects

In this experiment, the subject looked through the bioptic telescope at targets at various distances (without a laser pointer). Tracking results are shown in Fig. 12. The estimated aiming point was computationally shifted to compensate for the average scene camera parallax error (as explained in Section II-D and Fig. 7). Three subjects performed the same experiment, with average errors of 1.29°, 0.75°, and 0.93°. Note that such a compensation shift can make parallax errors for larger distances (expected to be relevant in driving situations) even smaller.

To test that the calibration can be performed by an experimenter for a visually impaired driver, the experiment was
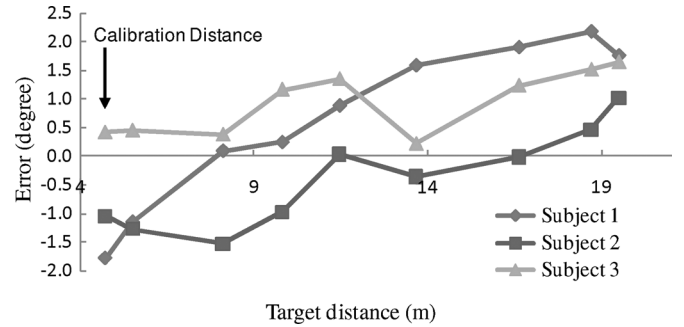

Fig. 12.   For a particular calibration distance (5 m), the tracking error of subject 1 (the experimenter who performed the calibration, diamonds), subject 2 (squares), and subject 3 (triangles), viewing a target at several distances from 2 to 20 m away with the bioptic telescope. The camera's parallax error is shifted to null at 8 m using method in Fig. 7. The average (unsigned) error was 1.29°, 0.75°, and 0.93° for subjects 1–3, respectively.

conducted with subjects 2 and 3 wearing the same telescope and using the calibration data established by subject 1 (the experimenter). These errors include random alignment error between subjects, as subjects may judge the center of the telescope slightly differently. As anticipated, the calibration data from the experimenter was valid for other subjects, since the same bioptic spectacle frame was tracked, and the camera placements were unchanged. So after calibration is completed by anyone who wears the subject's bioptic spectacles when the recording system is installed in a car, it is a calibration free tracking system for all subsequent use of those spectacles in that car.

E.   On-Road Results

We installed the tracking system in a car, using two side-by-side scene cameras to provide a horizontally wide view ($88° \times 33°$) while maintaining high image resolution. A day after one of the authors (GL) performed a calibration procedure, he drove through downtown Boston wearing the bioptic telescope, without further recalibrating. He looked through the telescope on several occasions, some of which were while the car was moving. The objects spotted through the telescope were noted. The recorded videos were processed to show the telescope aiming points over the video. All other experimenters were able to determine correctly what the driver looked at in all the noted occasions. Fig. 13 illustrates one of the bioptic use events, when the car stopped at an intersection. The track of the telescope aiming point is superimposed on the scene image. It clearly shows that the driver was checking the status of the two traffic lights using the telescope.

IV.   CONCLUSION

We have successfully developed and implemented a video surveillance system which can record usage of a bioptic telescope by vision-impaired drivers in their own cars and can provide a driving evaluator the estimated aiming point of the telescope superimposed on a view of the road and traffic scene. A novel calibration procedure was developed that needs to be performed only once with the driver's bioptic spectacles in the driver's car. The procedure is simple enough for low-vision drivers to perform, and we have shown that an experimenter can

Fig. 13. A trace of the calculated telescope aiming points while the driver was stopped for a red light. It clearly shows that the driver monitored the lights through the bioptic telescope. The inset, on the lower right of the left camera image, is added here to reveal the area obscured by the dense aiming points.

perform the calibration for the patients. Although the method still leaves some parallax related errors uncorrected, tests and computations showed that the system can achieve its required accuracy within a normal range of driver's head and body movements.

In planned studies, the system will provide valuable objective data to help us better understand how bioptic telescopes are used in normal driving. We expect to establish associations between certain patterns of bioptic use and driving performance (as judged by specialized driving instructors reviewing the recorded data) and, based on those data and analyses, to develop evidence-based training programs. All of this would not be possible if we do not know what bioptic drivers look at through their telescopes and when they use telescopes. In a pilot study using an analog VCR system (with no ability to determine bioptic aiming point) we already found that such data can be valuable. We were able to determine two bioptic drivers' frequency and time length of telescope usage in driving [19]. We found that their actual time viewing through the telescope was 60 times and 4 times less, respectively, than that reported by them in a prior survey study [3]. Such large errors in self-reporting underscore the importance of the objective data collection techniques that our telescope tracking system will facilitate.

ACKNOWLEDGMENT

REFERENCES

[1] N. Congdon, B. O'Colmain, C. C. Klaver, R. Klein, B. Munoz, D. S. Friedman, J. Kempen, H. R. Taylor, and P. Mitchell, "Causes and prevalence of visual impairment among adults in the United States," *Arch. Ophthalmol.*, vol. 122, pp. 477–485, Apr. 2004.

[2] E. Peli and D. Peli, *Driving With Confidence: A Practical Guide to Driving With Low Vision*. Singapore: World Scientific, 2002.

[3] A. R. Bowers, D. H. Apfelbaum, and E. Peli, "Bioptic telescopes meet the needs of drivers with moderate visual acuity loss," *Invest. Ophthalmol. Vis. Sci.*, vol. 46, pp. 66–74, Jan. 2005.

[4] J. G. Strong, J. W. Jutai, E. Russell-Minda, and M. Evans, "Driving and low vision: An evidence-based review of rehabilitation," *J. Vis. Impairment Blindness*, vol. 102, pp. 410–419, Jul. 2008.

[5] B. J. M. Melis-Dankers, A. C. Kooijman, W. H. Brouwer, R. B. Busscher, R. A. Bredewoud, P. H. Derksen, A. Amersfoort, M. A. M. Ijsseldijk, G. W. van Delden, T. H. P. A. Grotenhuis, and J. M. D. Witvliet, "A demonstration project on driving with reduced visual acuity and a bioptic telescope system in the Netherlands," *Vis. Impairment Res.*, vol. 10, pp. 7–22, Jun. 2008.

[6] C. Owsley and G. McGwin, Jr., "Vision impairment and driving," *Survey Ophthalmol.*, vol. 43, pp. 535–550, 1999.

[7] A. L. Corn, O. Lippmann, and M. C. Lewis, "Licensed drivers with bioptic telescopic spectacles: User profiles and perceptions," *Review*, vol. 21, pp. 221–230, 1990.

[8] C. Huss and A. Corn, "Low vision driving with bioptics: An overview," *J. Vis. Impairment Blindness*, pp. 641–653, Oct. 2004.

[9] F. Wallhoff, M. AblaBmeier, and G. Rigoll, "Multimodal face detection, head orientation and eye gaze tracking," in *IEEE Int. Conf. Multisensor Fusion Integration Intell. Syst.*, 2006, pp. 13–18.

[10] D. Beymer and M. Flickner, "Eye gaze tracking using an active stereo head," in *Proc. IEEE Comput. Soc. Conf. Comput. Vis. Pattern Recognit.*, 2003, pp. 451–458.

[11] J. Y. Kaminski, A. Shavit, D. Knaan, and M. Teicher, " Head orientation and gaze detection from a single image," in *Int. Conf. Comput. Vis. Theory Appl.*, Setubal, Portugal, 2006, pp. 85–92.

[12] C. Cudalbu, B. Anastasiu, R. Radu, R. Cruceanu, E. Schmidt, and E. Barth, "Driver monitoring with a single high-speed camera and IR illumination," in *Int. Symp. Signals, Circuits Syst.*, 2005, pp. 219–222.

[13] S. Shih, Y. Wu, and J. Liu, "A calibration-free gaze tracking technique," in *Proc. 15th Int. Conf. Pattern Recognit.*, 2000, pp. 201–204.

[14] J.-G. Wang and E. Sung, "Pose determination of human faces by using vanishing points," *Pattern Recognit.*, vol. 34, pp. 2427–2445, 2001.

[15] T. Horprasert, Y. Yacoob, and L. S. Davis, "Computing 3-D head orientation from a monocular image sequence," in *Proc. 2nd Int. Conf. Automatic Face Gesture Recognit.*, 1996, pp. 242–247.

[16] A. Tomono, M. Iida, and K. Ohmura, "Eye tracking image pickup apparatus for separating noise from feature portions," U.S. Patent 5 016 282.

[17] Y. Kondou and Y. Ebisawa, "Easy eye-gaze calibration using a moving visual target in the head-free remote eye-gaze detection system," in *IEEE Int. Conf. Virtual Environ., Human-Computer Interfaces, Measurement Syst.*, Jul. 2008, pp. 145–150.

[18] G. Luo, X. Fu, and E. Peli, "A recording and analysis system of bioptic driving behaviors," in *Proc. 5th Int. Driving Symp. Human Factors in Driver Assessment, Training, Vehicle Design; Driving Assessment*, Big Sky, MT, 2009, pp. 460–467.

[19] G. Luo and E. Peli, "Application of video surveillance systems to reveal actual use of bioptic telescopes in driving," presented at the Vision 2008, Montreal, QC, Canada, 2008.

Xianping Fu received the Ph.D. degree in communication and information system from Dalian Maritime University, Dalian, China, in 2005.

Since 2003, he is an Associate Professor in Information Science and Technology College, Dalian Maritime University, Dalian, China. From 2008 to 2009 he was a Postdoctoral Fellow at Schepens Eye Research Institute, Harvard Medical School, Boston, MA. His research interests include perception of natural scenes in engineering systems, including multimedia, image/video processing, and object recognition.
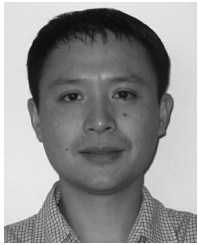
Gang Luo received the Ph.D. degree from Chongqing University, Chongqing, China, in 1997.

He is an investigator at Schepens Eye Research Institute and an instructor of ophthalmology at Harvard Medical School. He has been working in the fields of image processing and optics. His primary research interest is to apply his engineering expertise in low-vision rehabilitation. He is also interested in vision science. He has been peer-reviewers for multiple journals across engineering and vision science.

Eli Peli received the B.S.E.E. and the M.S.E.E. degrees from the Technion-Israel Institute of Technology, Haifa, Israel, and the OD degree from New England College of Optometry, Boston, MA.

He is the Moakley Scholar in Aging Eye Research and Co-Director of Research at Schepens Eye Research Institute, and Professor of Ophthalmology at Harvard Medical School, Boston, MA. He also serves on the faculty of the New England College of Optometry and Tufts University School of Medicine. Since 1983, he has been caring for visually impaired patients as the Director of the Vision Rehabilitation Service at Tufts Medical Center Hospitals, Boston, MA. His principal research interests are image processing in relation to visual function and clinical psychophysics in low-vision rehabilitation, image understanding and evaluation of display–vision interaction. He also maintains an interest in oculomotor control and binocular vision.

Dr. Peli is a Fellow of the American Academy of Optometry, the Optical Society of America, of the International Society of Optical Engineering (SPIE) and the Society for Information Display (SID). He is an Associate Editor of the IEEE TRANSACTIONS ON IMAGE PROCESSING.